

Molecular Hydrogen in the Lagoon: H₂ line emission from Messier 8

Michael G. Burton^{1,2}

¹ School of Physics, University of New South Wales, Sydney, NSW 2052

² School of Cosmic Physics, Dublin Institute for Advanced Studies, 5 Merrion Square, Dublin 2, Ireland

M.Burton@unsw.edu.au

Abstract

The 2.12 μm $v=1-0$ S(1) line of molecular hydrogen has been imaged in the Hourglass region of M8. The line is emitted from a roughly bipolar region, centred around the O7 star Herschel 36. The peak H₂ 1–0 S(1) line intensity is $8.2 \times 10^{-15} \text{ erg s}^{-1} \text{ cm}^{-2} \text{ arcsec}^{-2}$. The line centre emission velocity varies from -25 km s^{-1} in the SE lobe to $+45 \text{ km s}^{-1}$ in the NW lobe. The distribution is similar to that of the CO J=3–2 line. The H₂ line appears to be shock-excited when a bipolar outflow from Herschel 36 interacts with the ambient molecular cloud. The total luminosity of all H₂ lines is estimated to be $\sim 16 L_{\odot}$ and the mass of the hot molecular gas $\sim 9 \times 10^{-4} M_{\odot}$ (without any correction for extinction).

Keywords: infrared: ISM—ISM: HII regions—ISM: individual (M8)—ISM: molecules—molecular processes—shock waves—stars: formation.

1 Introduction

The Lagoon Nebula, Messier 8, is an HII region centred on the stellar cluster NGC 6523. It is embedded within a molecular cloud which extends to the young ($\sim 2 \times 10^6$ years old) star cluster NGC 6530, $10'$ to its east (Lada et al. 1976). Star formation is presumed to have proceeded from NGC 6530 and is now active in M8. Within M8's core lies the O7V star Herschel 36 (Woolf 1961), which has created a blister-type HII region, the Hourglass. This visually distinctive nebula is extended $15''$ EW and $30''$ NS, and lies $15''$ E of Herschel 36. The Hourglass is embedded within an extended HII region, $\sim 3'$ in extent, which is ionized by two O stars, HD 165052 and 9 Sgr (Woolf 1961, Lada et al. 1976). Nearby to Herschel 36 are a number of obscured sources, first observed in the near-IR by Allen (1986). Woodward et al. (1990) have designated them KS1 to KS5. Together, they may form a cluster of hot stars, analogous to the Trapezium in the Orion Nebula (M42), where θ^1_c Ori is the dominant member. In the mid-IR MSX¹ sky survey, this region appears as bright, extended source, with a $21 \mu\text{m}$ continuum flux of 960 Jy . This source is also prominent in sub-mm (Tothill 1999) and mm (Richter, Stecklum & Launhardt 1998) wavelength continuum. Nearby to Herschel 36, narrow band optical imaging with the HST reveals an object

¹see <http://irsa.ipac.caltech.edu/> for details.

pointed towards Herschel 36 (Stecklum et al. 1998). It is presumed to be an externally ionized circumstellar disk. These authors also estimate the distance to M8 to be 1.8 kpc, based on the association with NGC 6530.

Of particular interest to this paper are the observations by White et al. (1997) of intense CO line emission from M8. They found the peak CO J=3–2 intensity to be over 100 K, making it the second brightest CO line source known. The CO J=3–2 and 4–3 lines were mapped and found to have a loose, bipolar structure, extending NW–SE from Herschel 36. Taking the broad CO line profiles (extending over 20 km s^{-1}), and the presence of a jet-like object extending $0.5''$ SE of Herschel 36 in HST images (Stecklum et al. 1995), it seems likely that there is a molecular outflow in the core of M8. If so, it would be expected for there to be molecular hydrogen line emission as well, both shocked (from the deceleration of the outflow by the ambient cloud) and fluorescent (excited by far-UV photons from Herschel 36). However, White et al. (1997) also searched for the near-IR H_2 $v=1-0$ S(1) line in M8, but did not detect it. In this paper we report more sensitive observations for H_2 emission from M8, and find that there is indeed excited H_2 line emission from this source.

2 Observations and Data Reduction

The Hourglass region of the Lagoon Nebula, Messier 8, was imaged on 1997, July 22, using the IRIS 1–2.5 μm camera, in conjunction with the University of New South Wales Infrared Fabry-Pérot etalon (UNSWIRF, Ryder et al. 1998), on the 3.9-m Anglo Australian Telescope (AAT). The UNSWIRF etalon has a FWHM spectral resolution of $\sim 75 \text{ km s}^{-1}$, a pixel size of $0.77''$ and a $100''$ circular field of view. It is scanned through a spectral line of interest in order to obtain an emission line image of a source, with minimal contamination from any continuum radiation present. It also permits limited kinematic information to be obtained, through the emission velocity of the line centre across the field of view.

The H_2 1–0 S(1) (2.1218 μm) line was observed. Following a rapid scan to determine the plate spacing for the line centre, three on-line plate spacings were used for imaging, spaced by 39 km s^{-1} , together with an off-line setting, 840 km s^{-1} to the blue. Integration times were two minutes per plate spacing, and in addition, a sky frame, $300''$ N, was obtained immediately after each source frame.

The star BS 6748 (K=4.57 mags.) served as the flux standard, and was imaged at each etalon spacing. The absolute accuracy in flux calibration using a Fabry-Pérot etalon is around 30%. A diffused dome lamp provided a flat field for each etalon spacing. An arc lamp was scanned through a free spectral range in order to wavelength calibrate the etalon response for each pixel of the array.

Data reduction was undertaken using a custom software package using IRAF². Frames are linearised, flat-fielded using a dome flat at the appropriate plate spacing, cleaned of bad pixels, sky-subtracted, shifted to align stars in each frame, smoothed and the off-line frame subtracted from each on-line frame (having been appropriately scaled to minimise residuals from the subtraction process). Stacking of the three on-line frames produces a data cube, which is fitted, pixel-by-pixel, with the instrumental profile (a Lorentzian), to yield a line image. A coordinate frame was added using the digitised sky survey³ to relate common stars between the visible and 2.1 μm .

The line centre at each pixel position is obtained from the plate spacing determined for the

²Image Reduction and Analysis Facility (see <http://www.iraf.noao.edu>).

³see <http://stdatu.stsci.edu/dss/>.

well as with the S/N the line is measured with. Where this is adequate, the accuracy typically is $\sim 10 \text{ km s}^{-1}$. Absolute line emission velocities were determined with reference to the plate spacing found for the peak of the H_2 emission in M17, which is assumed to be at $+21 \text{ km s}^{-1}$ (V_{LSR}). Note that, as a consequence of the broad wings to the instrumental profile, the line width cannot be determined unless it is very much wider than the spectral resolution (which it is not in M8).

3 Results

The field surrounding the Hourglass is shown in the 3-colour near-IR image in Fig. 1. The J ($1.25 \mu\text{m}$), H ($1.65 \mu\text{m}$) and K ($2.2 \mu\text{m}$) images were previously obtained by the author and David Allen during the commissioning of IRIS in 1991. They have been combined to produce a 3-colour image which simulates the appearance of the nebula if our eyes were sensitive to the $1\text{--}2.5 \mu\text{m}$ wavelength range. Embedded and obscured stars are red or yellow and foreground stars are blue. The HII region of the Hourglass appears blue as its near-IR emission is dominated by Paschen lines of hydrogen in the J-band. The morphology of the Hourglass is the same in the three bands, suggesting that this is its intrinsic shape, rather than being determined by variable extinction in the optical (as suggested by Woodward et al. 1986). In the figure, Herschel 36 and the Hourglass are marked, as well as the four $2 \mu\text{m}$ sources KS1–KS4 (Woodward et al. 1990).

The molecular hydrogen $v=1\text{--}0$ (1) line emission image of M8 is shown in Fig. 2, overlaid with contours of the line flux. The emission is clumped and the morphology broadly bipolar, centred about Herschel 36. Also shown are the line centre velocities for selected locations, obtained from fitting the instrumental profile to the three on-line images. While the accuracy of individual velocities is no better than $\sim 10 \text{ km s}^{-1}$, they do indicate that there is a velocity gradient of $\sim 70 \text{ km s}^{-1}$ across the field, extending from $\sim -25 \text{ km s}^{-1}$ to the east of Herschel 36, to $\sim +45 \text{ km s}^{-1}$ to its north-west.

The $2.12 \mu\text{m}$ H_2 line emission is compared to the $2.2 \mu\text{m}$ K-band continuum emission in Fig. 3. It can be seen that the H_2 emission peaks close to the continuum peak, Herschel 36. The Hourglass, however, appears as a cavity in the H_2 distribution. H_2 line fluxes have been determined for the apertures indicated in this figure, and are listed in Table 1, together with the positions of the emission peaks. The total $1\text{--}0 \text{ S}(1)$ line emission from the region is $1.0 \times 10^{-11} \text{ erg s}^{-1} \text{ cm}^{-2}$ and the peak intensity is $8.2 \times 10^{-15} \text{ erg s}^{-1} \text{ cm}^{-2} \text{ arcsec}^{-2}$. At an assumed distance of 1.8 kpc for M8, these figures are equivalent to a luminosity in the $1\text{--}0 \text{ S}(1)$ line of $1.1 L_{\odot}$, and to a peak column density in the $(v,J) = (1,3)$ level of the H_2 molecule of $1.4 \times 10^{16} \text{ cm}^{-2}$ (without any correction applied for extinction to the emitting region).

An enlarged image of the H_2 line emission, overlaid on the K-band continuum, is shown in Fig. 4. It is apparent that the H_2 emission does not, in fact, peak at the location of Herschel 36. The H_2 emission peaks approximately ($1.5''\text{E}$, $0.5''\text{S}$) from Herschel 36, roughly half way between it and the proplyd ($2.5''\text{E}$, $1.5''\text{S}$) of Herschel 36.

4 Discussion

4.1 H_2 Morphology and Kinematics

Given the intensity of the CO line emission measured in M8 by White et al. (1997), it was a considerable surprise when the same authors failed to detect any H_2 line emission from the source. M8 is the second most intense CO source detected, and clearly a site of active massive star

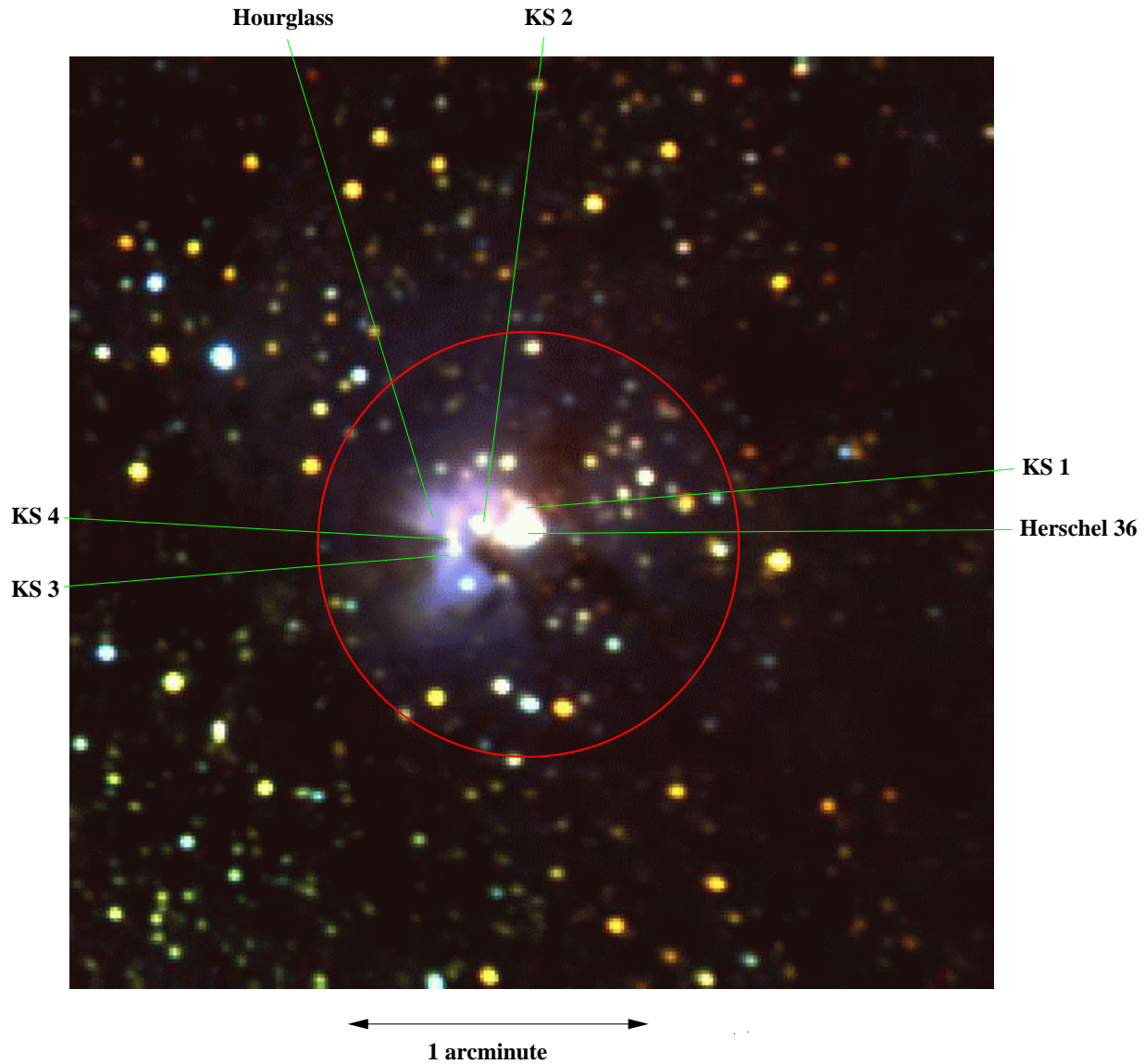


Figure 1: Three-colour near-infrared image of Messier 8. Blue denotes the J ($1.25\,\mu\text{m}$) band, green the H ($1.65\,\mu\text{m}$) band and red the K ($2.2\,\mu\text{m}$) band. The field imaged with UNSWIRF is indicated by the red circle. Several features of interest are labelled; Herschel 36 the O7V star powering the HII region emission, the near-IR sources KS1 to KS4, and the Hourglass. Heavily reddened stars appear red or yellow and foreground stars blue. The Hourglass is blue because the near-IR emission is dominated by Paschen recombination lines of hydrogen in the J-band. The scale bar shows an angular distance of 1 arcminute.

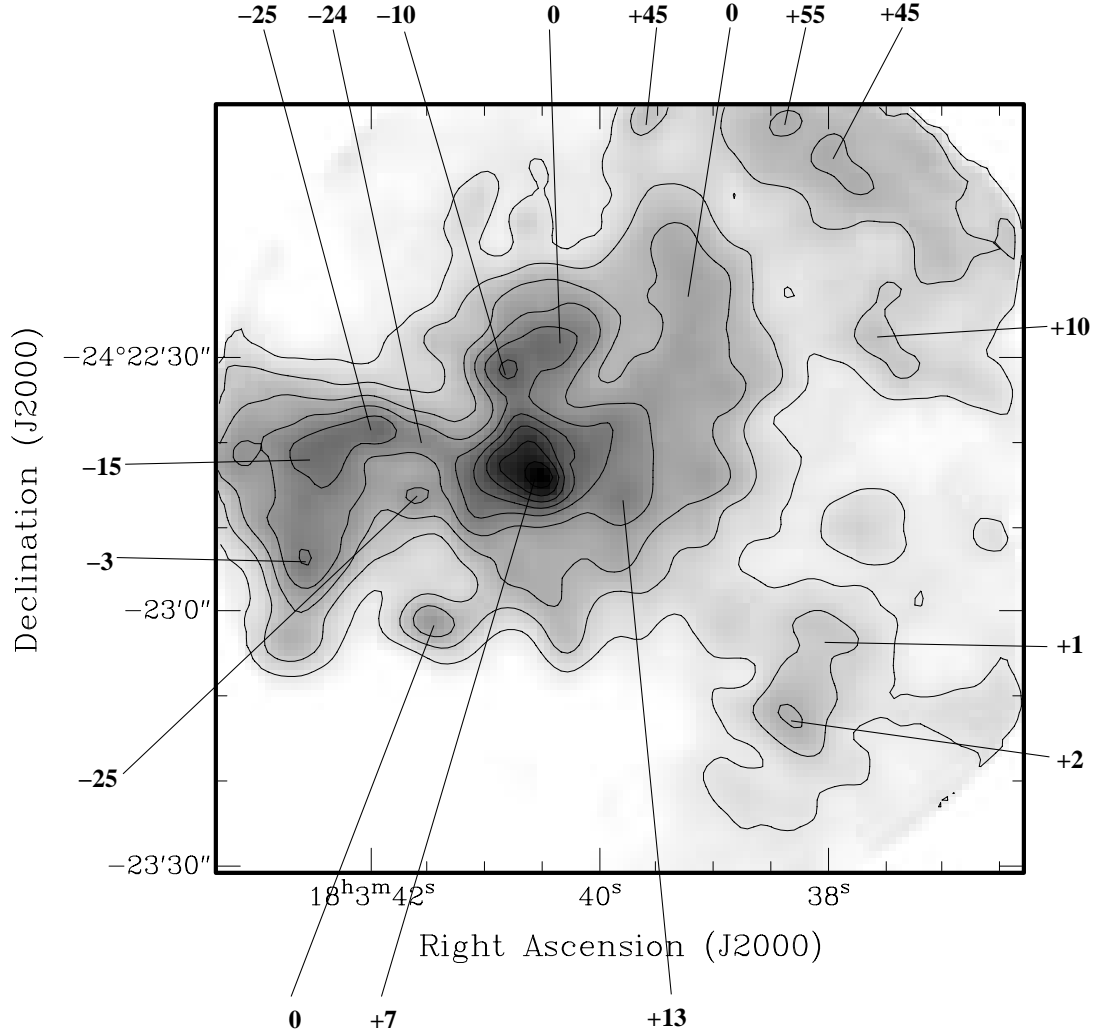


Figure 2: Image of the molecular hydrogen $v=1-0$ S(1) line emission at $2.12\mu\text{m}$ in Messier 8, overlaid with contours of the line emission. Contours start at, and are in steps of, $8.5 \times 10^{-16} \text{ erg s}^{-1} \text{ cm}^{-2} \text{ arcsec}^{-2}$. Also indicated are the H₂ line centre velocities, in km s^{-1} (V_{LSR}), at selected locations.

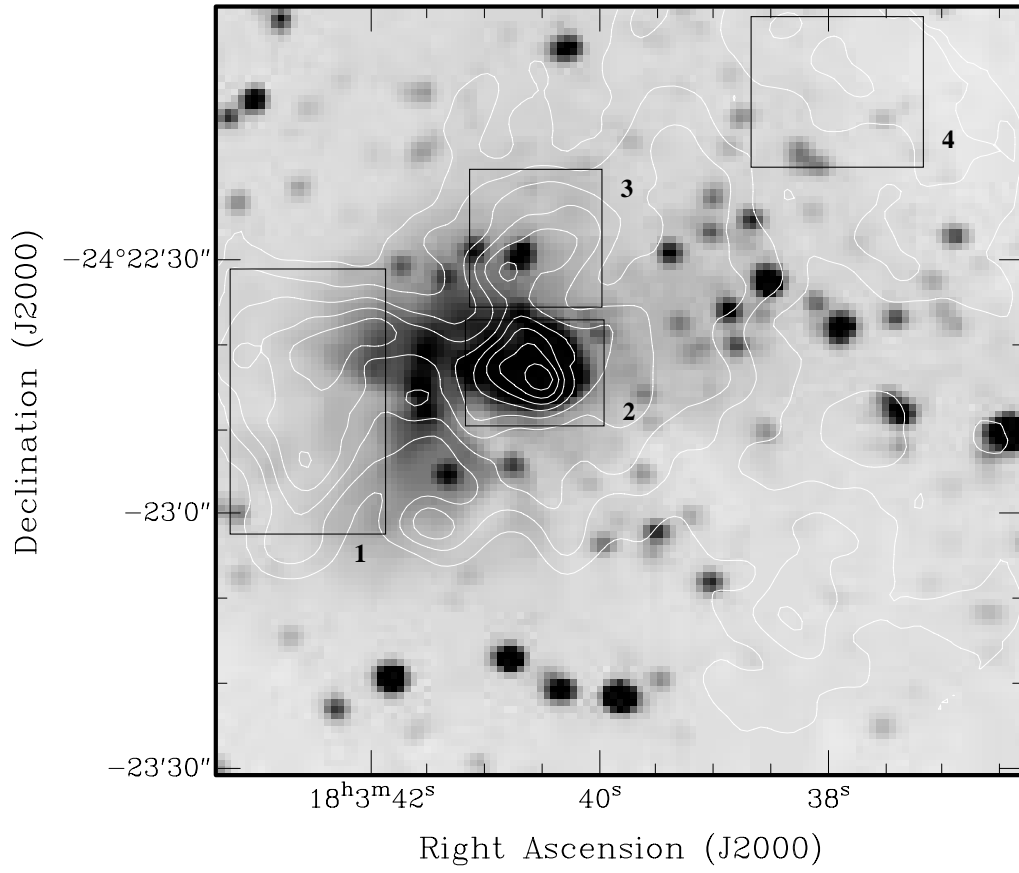


Figure 3: Image of the K-band ($2.2\,\mu\text{m}$) continuum emission from M8, overlaid with contours of the H_2 1–0 S(1) $2.12\,\mu\text{m}$ line emission. Contours are as in Fig. 2. The numbered boxes refer to the apertures in Table 1.

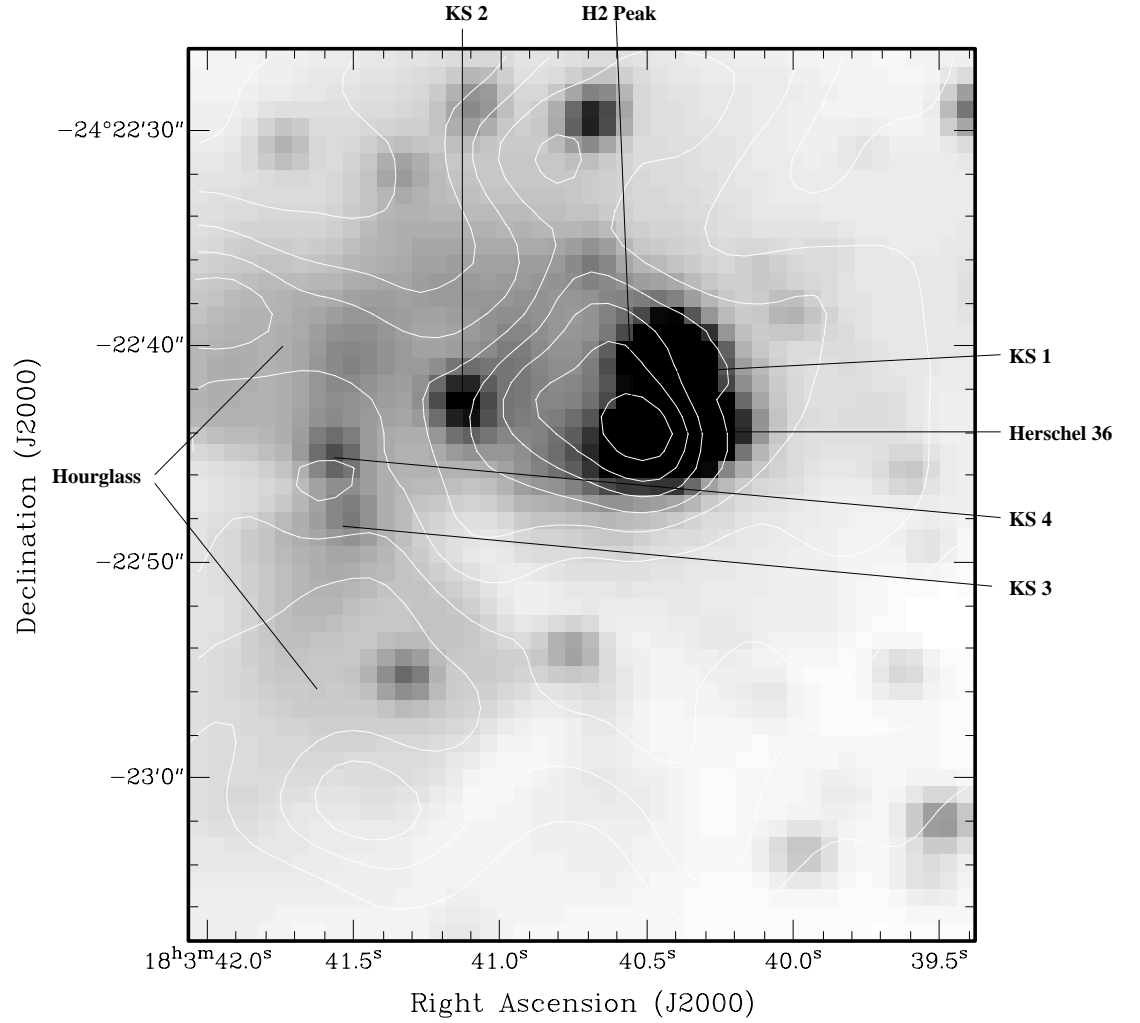


Figure 4: Enlarged image of the central region of M8, showing the K-band continuum, overlaid by contours of the H₂ 1-0 S(1) line emission. Contour levels are as in Figs. 2 and 3. The separation between the H₂ peak and Herschel 36, the exciting star for the Hourglass, is apparent. These features are labelled, together with the infrared sources KS1-KS4.

Region ¹	RA ² 18 ^h 03 ^m	Dec ² −24°22′	Aperture ³ arcsec	1–0 S(1) Flux ⁴ ×10 ^{−13} erg s ^{−1} cm ^{−2}	1–0 S(1) Peak Intensity ⁵ ×10 ^{−15} erg s ^{−1} cm ^{−2} arcsec ^{−2}
1	42.5 ^s	22″	22 × 32	17.6 ± 0.1	4.8 ± 0.5
2	40.5 ^s	44″	17 × 13	11.1 ± 0.1	8.2 ± 0.5
3	40.8 ^s	31″	17 × 17	9.2 ± 0.1	5.3 ± 0.5
4	38.4 ^s	02″	20 × 22	7.8 ± 0.1	2.7 ± 0.5
Total ⁶	40.5 ^s	44″	89 × 79	102 ± 3	8.2 ± 0.5

¹ Aperture, as shown in Fig. 3.

² Position of peak emission within the aperture, in J2000.

³ Size of aperture.

⁴ Total H₂ 1–0 S(1) line emission from aperture.

⁵ Peak emission intensity within aperture.

⁶ Integrated fluxes for the entire field.

formation. White et al. imaged M8 through a narrow band (1% width) filter centred on the H₂ 1–0 S(1) line, and used a broad band 2.2 μ m image to subtract the continuum from it. They failed to detect any H₂ line emission, and placed an upper limit of $\leq 3.4 \times 10^{-4}$ erg s^{−1} cm^{−2} sr^{−1} on the line flux. This is equivalent to $\leq 8 \times 10^{-15}$ erg s^{−1} cm^{−2} arcsec^{−2}, equal to the peak intensity we actually measured in M8. Thus, the upper limit of White et al. (1997) is consistent with our detection of H₂ line emission. It does, however, highlight the difficulty of measuring line emission through narrow band filters in the presence of a strong continuum, and the advantages of using a Fabry-Pérot etalon for such measurements. The 1 σ detection limit we achieved, with just 6 minutes on-line integration, is 3×10^{-16} erg s^{−1} cm^{−2} arcsec^{−2}.

Comparison with the ¹²CO J=3–2 image obtained by White et al. (1997) (see their Fig. 2a, within the outermost white contour, at a level of 230 K km s^{−1}) shows that the morphology is very similar to the H₂ 1–0 S(1) line, given the difference in resolution of the two images (the CO 3–2 image was obtained through a 14″ beam). The line emission is peaked around Herschel 36, and extends in two lobes in a NW–SE, $\sim 45''$ from the centre. The extension to the SW is also seen in both line images. This corresponds to a region of increased extinction seen in optical images.

The CO 3–2 line also displays broad line profiles, extending from +2 to +22 km s^{−1} (V_{LSR}), and peaking at +10 km s^{−1} near Herschel 36. Profiles in the NW lobe tend to extend somewhat further to the red than they do in the SE lobe. Similar behaviour is displayed by the H₂ line centre velocities, though the velocity extent is considerably larger than for the CO line. The H₂ velocity ranges from ~ -25 km s^{−1} in the SE lobe, to +7 km s^{−1} at the emission peak, to $\sim +45$ km s^{−1} in the NW lobe.

4.2 Shock Excitation

High spatial resolution imaging in the optical lines of H α and [SII] with the HST, and with adaptive optics in the K and L band near-IR continuum (Stecklum et al. 1995) shows an ionized, jet-like feature, extending $\sim 0.5''$ from Herschel 36 to the SE (the K and L band emission is presumed to dominated by the 2.16 μ m Br γ and 4.05 μ m Br α hydrogen recombination lines). Taken with the morphology and velocity extent of both the CO and H₂ line emission, this suggests that the

Herschel 36 with the ambient molecular cloud. The H_2 morphology then represents the location where a loosely collimated bipolar flow from Herschel 36, surrounding an ionized jet, runs into a molecular cloud. The larger velocities seen in H_2 than CO represent the shock speeds where the outflow impacts the molecular cloud. The flow then cools and decelerates, and this compressed gas is seen in the lower-velocity CO lines.

Presuming the H_2 line emission is dominated by shocks, it is possible to estimate the total H_2 line luminosity and the mass of hot, post-shock gas. In molecular shocks, the total H_2 line luminosity is typically ~ 15 times the 1–0 S(1) line flux, and the fraction of hot H_2 that is in the $(v,J)=(1,3)$ state of the molecule is $\sim 2\%$ (e.g. see Burton 1992). The total H_2 line luminosity from the source is then $\sim 16 L_\odot$, and the peak column density of hot H_2 is $6.1 \times 10^{17} \text{ cm}^{-2}$ (i.e. at the emission peak). The total mass of hot H_2 in the source is $\sim 9 \times 10^{-4} M_\odot$. These figures should be corrected for an unknown amount of extinction to the emitting region. This cannot be obtained from our data, so we will use the estimates of $A_v \sim 5$ mags. towards Herschel 36 and the proplyd, made by Stecklum et al. (1998). This is equivalent to ~ 0.5 mags. at $2.1 \mu\text{m}$. If this is representative of the extinction to the H_2 emitting region, then the extinction-corrected luminosity, peak column density and mass of hot H_2 are $\sim 25 L_\odot$, $\sim 10^{18} \text{ cm}^{-2}$ and $\sim 1.5 \times 10^{-3} M_\odot$, respectively.

These figures can be compared to the total amount of molecular gas and its peak column density, estimated by White et al. (1997) from the CO lines. They determined these to be $\sim 31 M_\odot$ and $1.3 \times 10^{23} \text{ cm}^{-2}$, respectively. These are very much greater than the quantities determined for the hot molecular gas, as expected if the hot material comprises just a thin skin of material in front of cooled, compressed gas. The cooling time for hot H_2 , τ_{cool} , is ~ 1 year, which therefore suggests that the outflow must have existed for $\sim 10^{4-5}$ years.

The mechanical luminosity of the outflow can be estimated as

$$L_{\text{mech}} \sim 0.5 M_{\text{hot}} V^2 / \tau_{\text{cool}}, \quad (1)$$

where M_{hot} is the mass of hot H_2 and V is the average speed of the shock wave. Taking this to be 35 km s^{-1} (half the range in velocity of the H_2 line emission) yields $L_{\text{mech}} \sim 300 L_\odot$ (extinction corrected), an order of magnitude greater than the H_2 line luminosity. This is obviously a crude estimate, but it does indicate that the H_2 lines are a significant contributor, and possibly the dominant one (given the assumptions made), to the cooling of the gas behind the shock front.

4.3 Fluorescence

Despite our conclusion that the H_2 line emission is dominated by shocks, there may still be a significant contribution by far-UV fluorescence to parts of it. The Hourglass is an HII region, excited by the UV radiation from Herschel 36. The gap in the H_2 emission around the Hourglass suggests a physical connection between the two, for instance the Hourglass may be a cavity embedded within the outflow. The H_2 line velocity in the cavity covering the Hourglass is approximately constant, taking the value $\sim -25 \text{ km s}^{-1}$ (V_{LSR}). A constant velocity would be expected for fluorescent emission from a molecular cloud with small internal motions (e.g. see Burton et al. 1990). The velocity measured then indicates the V_{LSR} velocity of the surface of the photodissociation region. This velocity, -25 km s^{-1} , is at the negative limit of the 50 km s^{-1} range for the ionized gas in the Hourglass, as measured through [OIII] 5007Å line emission (Chakraborty & Anandarao 1999). Furthermore, Woodward et al. (1986) have detected $3.28 \mu\text{m}$ PAH emission from the region around the Hourglass. This is excited by the same far-UV photons that can fluorescently excite H_2 (e.g. see the PAH emission in NGC 6334; Burton et al. 2000). Therefore, it seems likely that some of

5 Conclusions

Strong near-IR molecular hydrogen line emission is produced from around the Hourglass in the M8 star forming region. The peak H_2 brightness is at the detection limit of a previous attempt to measure H_2 line emission from the source, thus explaining the reported non-detection. The H_2 is emitted from an extended, roughly bipolar region, centred on the powering source for the Hourglass, Herschel 36. It is orientated along a NW-SE direction. The morphology is similar to that of the CO J=3-2 distribution in M8. Taken with the $\sim 70 \text{ km s}^{-1}$ variation in the H_2 line centre across the region, and the 20 km s^{-1} width of the CO profiles, this suggests that the H_2 emission is shock-excited, when a bipolar outflow, originating from Herschel 36, impacts the surrounding molecular cloud. The total H_2 line luminosity is $\sim 16 L_\odot$ (not corrected for any extinction). The H_2 lines provide a significant means of ridding the source of the mechanical energy in the outflow, though we cannot yet determine whether H_2 line emission is the dominant coolant in the shocked gas.

To examine the excitation mechanism more closely, in particular to determine whether there may also be fluorescent H_2 emission, it would be necessary to measure higher excitation lines of the molecule, from $v \geq 2$. This could be done either by long-slit spectroscopy, or through further Fabry-Pérot imaging, with the waveplates tuned to appropriate lines. To improve the determination of the flow energetics it will be necessary to use greater spectral resolution and resolve the line profiles, in order to measure the momentum and kinetic energy distribution of the hot molecular gas across the source.

Acknowledgements

Several people have provided considerable assistance with the work presented here. I particularly wish to thank Michael Ashley, Lori Allen, Jung-Kyu Lee, Stuart Ryder and John Storey for their help with the observations. Christine Carmody also helped with the reduction of the data. The staff of the Anglo Australian Telescope provided great assistance with the installation and operation of UNSWIRF.

References

- Allen, D.A., 1986, MNRAS, 319, 35P.
- Burton, M.G., 1992, Aust. J. Phys., 45, 463.
- Burton, M.G., Ashley, M.C.B., Marks, R.D., Schinckel, A.E., Storey, J.W.V., Fowler, A., Merrill, M., Sharp, N., Gatley, I., Harper, D.A., Loewenstein, R.F., Mrozek, F., Jackson, J. & Kraemer, K., 2000, ApJ, 542, 359.
- Burton, M.G., Geballe, T.R., Brand, P.W.J.L. & Moorhouse, A., 1990, ApJ, 352, 625.
- Chakraborty, A. & Anandarao, B.G., 1999, A&A, 346, 947.
- Lada, C.J., Gull, T.R., Gottlieb, C.A. & Gottlieb, E.W., 1976, ApJ, 203, 159.
- Richter, S., Stecklum, B. & Launhardt, R., 1998, Abstracts of contributed talks and posters presented at the annual scientific meeting of the Astronomische Gesellschaft, Heidelberg, September 14-19, 1998.

- Stecklum, B., Henning, T., Eckart, A., Howell, R.R. & Hoare, M., 1995, ApJ, L153.
- Stecklum, B., Henning, T., Feldt, M., Hayward, T.L., Hoare, M.G., Hofner, P. & Richter, S., 1998, AJ, 115, 767.
- Tothill, N.F.H., 1999, PhD Thesis, Queen Mary and Westfield College, University of London.
- White, G.J., Tothill, N.F.H., Matthews, H.E., McCutcheon, W.H., Huidtgren, M. & McCaughrean, M.J., 1997, A&A, 323, 529.
- Woodward, C.E., Pipher, J.L., Helfer, H.L., Sharpless, S., Moneti, A., Kozikowski, A., Oliveri, M., Willner, S.P., Lacasse, M.G. & Herter, T., 1986, AJ, 91, 870.
- Woodward, C.E., Pipher, J.L., Helfer, H.L. & Forrest, W.J., 1990, ApJ, 365, 252.
- Woolf, N.J., 1961, PASP, 73, 206.

